JOURNAL OF MATERIALS SCIENCE **40** (2005) 1237– 1243

Crack growth in a new nickel-based superalloy at elevated temperature

Part III *Characterisation*

J. TONG*
Department of Mechanical and Design Engineering, University of Portsmouth, Anglesea Road, Anglesea Building, Portsmouth PO1 3DJ, UK

S. DALBY
Department of Mechanical and Design Engineering, University of Portsmouth, Anglesea Road, Anglesea Building, Portsmouth PO1 3DJ, UK; Astrium Ltd. Anchorage Road, Portsmouth PO3 5PU, UK

J. BYRNE
Department of Mechanical and Design Engineering, University of Portsmouth, Anglesea Road, Anglesea Building, Portsmouth PO1 3DJ, UK

Crack growth mechanisms at elevated temperature have been examined in a new nickel-based superalloy. Scanning electron microscopy has been used to identify the fracture modes in specimens tested under triangular, fast-slow, slow-fast, dwell and sustained loading conditions at 650 and 725°C. A model has been developed considering a predominant oxidation-driven crack growth mechanism, as revealed from the SEM analysis. An oxidation sensitive time has been adopted to characterise the rate-dependent crack growth, together with an Arrehenius relationship to take account of the influence of temperature. The model predictions have been compared with the experimental results.

1. Introduction

Crack growth at elevated temperature has been examined in a new nickel-based superalloy for four cyclic waveforms at 650 and 725°C, as presented in Part I [1] of this paper. The predominant mechanism appears to be a mixture of time and cycle dependent crack growth for majority of the cases studied. The effect of loading waveform on crack growth rate seems to be insignificant for base frequencies over 0.01 Hz, except in the fast-slow case. Frequency has been found to be inadequate in correlating the crack growth rates for all waveforms. A suitable parameter for characterisation purposes needs to be found.

Creep deformation has been found to be very limited from both experimental and numerical studies; likewise the role of crack closure has also been found to be largely irrelevant to the cases studied, as presented in Part II [2] of this paper. Our recent work [3] and the work of others [4–6] seem to suggest that oxidation appears to be the predominant crack driving force for nickel-based alloys at the intermediate temperature range. Potential candidates for characterisation purposes need therefore to reflect the essentially linear-elastic stress-strain fields near the crack tip and rate-dependent nature of the crack growth.

In this final part of the paper, the fracture mode and oxide morphology will be examined using scanning electron microscopy (SEM). The mechanisms of crack growth will be explored. Potential characterisation parameters will be evaluated where the mechanical variables identified in the experimental work will be explicitly incorporated. An oxidation sensitive time will be adopted in the model and the results from the analysis will be compared with the experimental data.

2. Mechanisms for crack growth

From the experimental results, the majority of the crack growth rate data seem to indicate a mixed cycle-time dependent crack growth, as illustrated by a slope of -0.3 to -0.4 in the log-log crack growth rate vs. frequency plots [1]. Even for crack growth under long dwell and sustained loading conditions, a slope of -1, which indicates pure time-dependent crack growth [7], has never been achieved, although the slope has noticeably increased at these extreme conditions, particularly at 725°C.

Predominant time dependent crack growth may be due to creep or environmental embrittlement due to oxidation. To establish the dominant fracture mechanism,

*Author to whom all correspondence should be addressed.

SEM has been employed to study the fracture modes with respect to the loading waveform at both temperatures. The influence of load level was removed by the ΔK-controlled testing method such that all micrographs taken were at a similar stress intensity level. A mixture of transgranular and intergranular crack growth was observed for all load cases, although the proportion of the transgranular crack growth decreased as the base frequency was reduced. No cavities in the vicinity of the crack tip or grain boundaries were observed in all cases studied, indicating the lack of creep deformation, consistent with the results from mechanical testing [1] and the numerical analysis [2]. Fig. 1 shows the micrographs of fracture surfaces of a specimen tested under triangular waveform at three different frequencies at $\Delta K = 30$ MPa$\sqrt{\text{m}}$ and 650°C. Typical features of a transgranular fracture can be observed at 0.25 Hz (a) with clearly visible striations that characteristic of time-independent fatigue crack growth. At 0.01 Hz, some striations are still visible, although the proportion is reduced with a fair amount of intergranular cracking. At 0.001 Hz, the fracture surface exhibits predominantly intergranular crack growth although, occasionally, striations are still present. The general morphology of the fracture surfaces seems to be consistent with the SEM micrographs with a smooth, flat surface at 0.25 Hz, as opposed to a much rougher surface at 0.001 Hz, while the roughness of the fracture surface at 0.01 Hz lies in between. It seems that as the frequency reduced, the proportion of the intergranular cracking increased. This pattern of variation in the roughness of the fracture surfaces was found to be typical for slow-fast and dwell as well as triangular waveforms at 650°C. The only exception was the case of fast-slow waveform where smooth, flat surfaces were observed at all frequencies and SEM revealed transgranular crack growth.

At 725°C, a similar pattern of variation in the fracture mode was observed, although the proportion of the intergranular crack growth was greater for the same base frequency than that at 650°C. Fig. 2 shows that at very low frequencies (a) or long dwell (b) cases, the fracture mode is decisively intergranular cracking and resembles the fracture surface under sustained load (c).

It is well known that nickel-based alloys are particularly susceptible to oxygen exposure at intermediate temperatures [8]. Oxide formation may reduce boundary mobility while oxygen diffusion prompts crack initiation and growth. The oxide deposits have been observed on the fracture surfaces of all specimens tested at both temperatures. The morphology of these deposits has been examined in a specimen tested under dwell loading at 725°C. The specimen was sectioned, polished and examined using FEGSEM [1]. The oxide layer was measured to assess the influence of the waveform and the test duration on the accumulation of oxides. There seems to be no discernable difference in the apparent oxide thickness for different periods of exposure to air (Fig. 3). The thickness of the oxide does not seem to vary with the prolonged hold at maximum load either [9]. It seems that the superficial oxides reached a saturated state once they accumulated to a certain level. This observation seems to

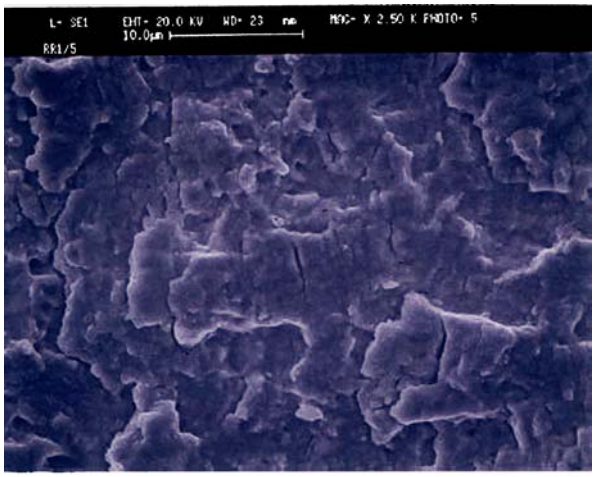

(a)

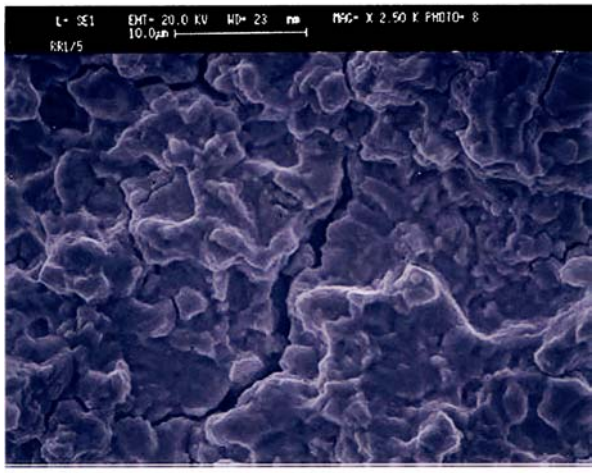

(b)

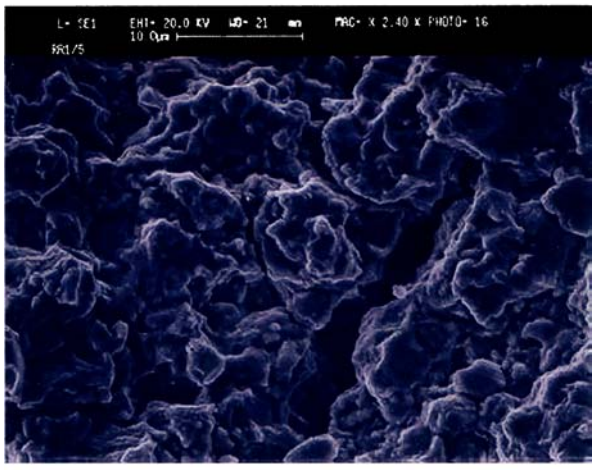

(c)

Figure 1 Fracture surfaces of a specimen tested under triangular waveform at 650°C, $\Delta K = 30$ MPa$\sqrt{\text{m}}$: (a) $f = 0.25$ Hz, (b) $f = 0.01$ Hz, and (c) $f = 0.001$ Hz.

be consistent with a two-stage oxidation mechanism [10], which suggests the formation of the initial nickel-based oxides, followed by a denser sublayer composed of chromia, Cr_2O_3. The completion of this Cr_2O_3 layer is regarded as an attainment of saturation. The time required to reach this stage is a function of temperature, oxygen partial pressure, and local stress/strain conditions. Since these parameters were maintained constant

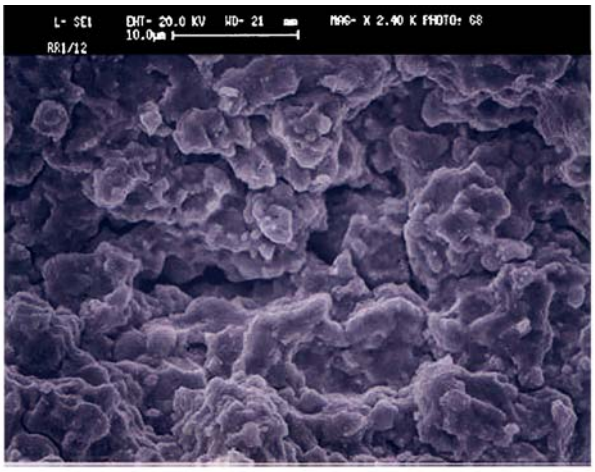

(a)

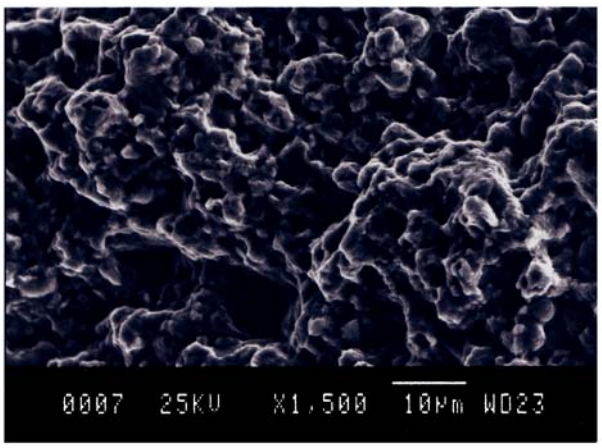

(b)

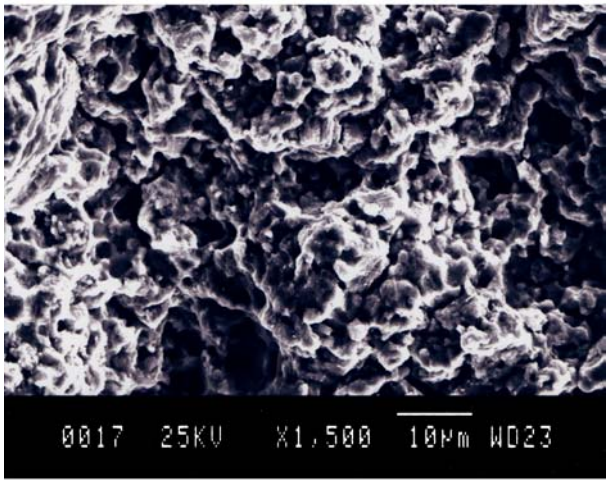

(c)

Figure 2 (a) Fracture surface of a specimen tested under triangular waveform at 0.001 Hz, 725°C, $\Delta K = 30$ MPa$\sqrt{}$m. (b) Fracture surface of a specimen tested under dwell loading (1-300-1-1) at 725°C, $\Delta K = 30$ MPa$\sqrt{}$m. (c) Fracture surface of a specimen tested under static loads at 725°C, $K_{max} = 33$ MPa$\sqrt{}$m.

during testing, the transition time would be the same for newly exposed crack surfaces. According to Ghonem and Zheng [5], at 650°C and atmospheric pressure, the time required for saturation to occur in nickel alloys is in the order of a few minutes, well above the present observation periods. Oxygen may diffuse along a preferential grain boundary path, promoting intergranular cracking. Hippsley *et al*. [11, 12] reported that stable crack growth occurred in a step-wise fashion due to the build-up of oxygen ahead of the crack tip and subsequent decohesion of the oxygen-enriched area. Very short times are required for oxygen to embrittle the area near the crack tip. Molins *et al*. [4] indicated that the time required to embrittle the local material is less than 20 s. Once the embrittlement is taken place through absorption and diffusion, accelerated crack growth may occur when the mechanical conditions at the crack tip are favourable.

The influence of loading frequency on oxidation driven crack growth has been studied by Ghonem and Zheng [13]. At high loading frequencies, homogeneous deformation, characterised by high slip density, results in strain accommodation and limited oxygen diffusion. At low frequencies, low slip density would promote grain boundary stress concentration, particularly if stress relief by grain boundary sliding is not permitted, such as in creep-brittle materials. The grain boundary diffusivity will increase hence promote intergranular fracture. As the loading frequency decreases, the degree of slip line homogeneity in the crack tip zone is reduced hence the intergranualar oxygen diffusion increases. The damage mode at the crack tip becomes a combination of oxidation and fatigue. The proportion of each component depends on the loading frequency alone at a given stress intensity level, as revealed from the present experimental results.

3. Characterisation

3.1. Correlation parameters

Base loading frequency seemed to correlate well with the crack growth rates obtained under symmetrical loading waveforms [14]. However, the correlation with the crack growth rate data from asymmetrical waveforms was poor [15]. Specifically, crack growth rates under fast-slow waveform maintained fairly constant for all loading frequencies at 650°C, and showed only some slight increase with the increase of the base frequency at 725°C, as shown in Fig. 4. The objective of this work was therefore to find a parameter that would correlate the crack growth rate data for asymmetrical as well as symmetrical waveforms at both 650 and 725°C. Loading time, $t_1 + t_2$, seems to be promising in correlating fast-slow and slow-fast data at 650°C, as shown in Fig. 5a. However, a variation by a factor of 5 in crack growth rates was found for the same correlation of data obtained at 725°C (Fig. 5b). Clearly at this higher temperature, the unloading time, as well as the loading time, has a notable impact on the crack growth and needs to be considered.

An oxidation sensitive time (OST), $0.9t_1 + t_2 + 0.1t_3$, has been adopted as the general correlation parameter. This parameter was chosen based on the work of Molins *et al*. [4] who studied the oxidation assisted fatigue crack growth in nickel-based superalloys by varying the oxygen partial pressure during a loading cycle. They found that oxidation effects occur primarily during the loading part of the cycle and part of the unloading cycle while the crack tip is in traction. The choice of an oxidation parameter seems to be appropriate considering both the experimental evidence [1] and

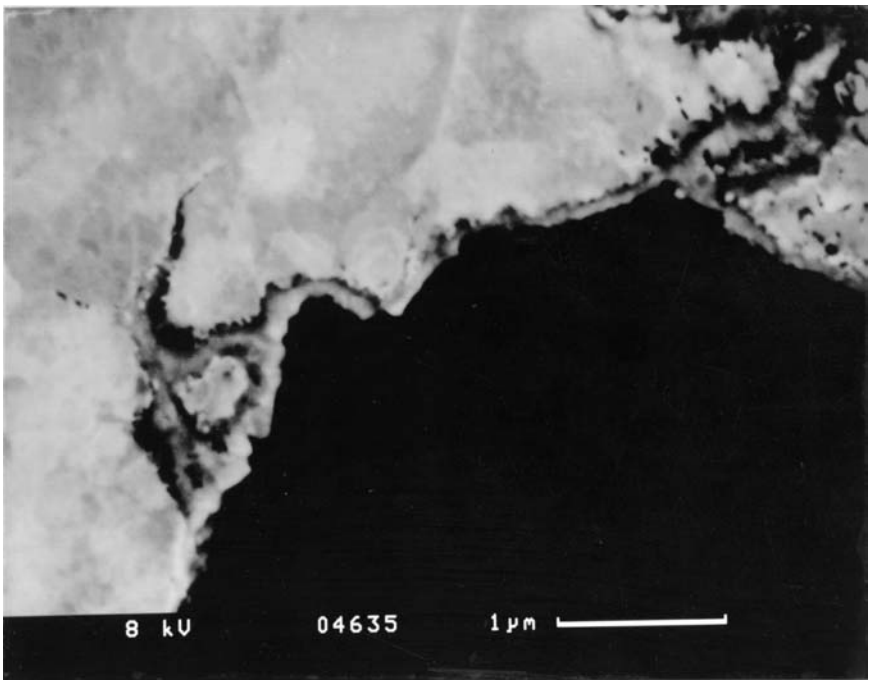

(a)

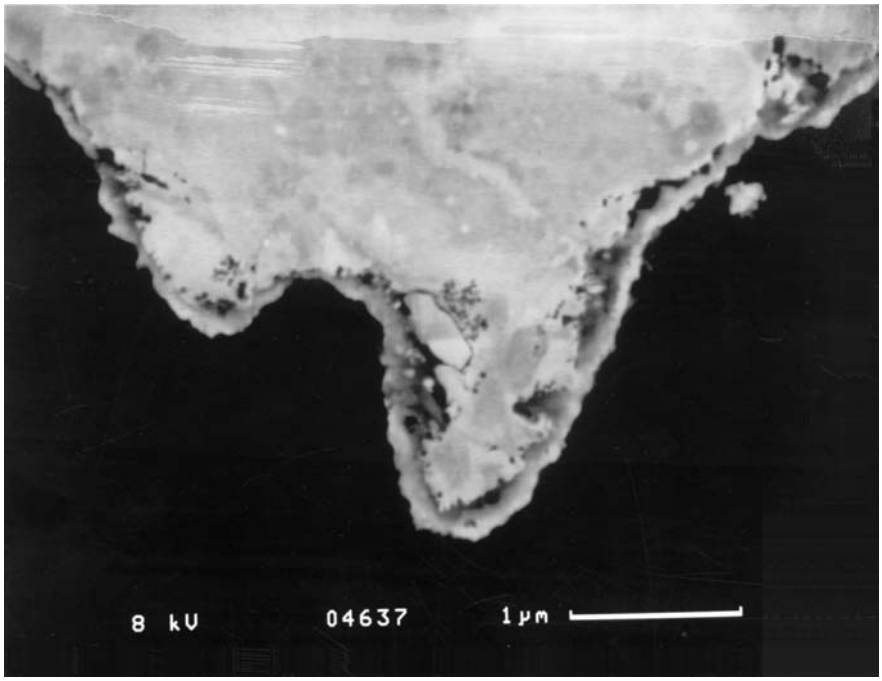

(b)

Figure 3 Oxide deposits on the fracture surfaces of samples tested at 725 °C, $\Delta K = 30$ MPa$\sqrt{}$m: (a) Short dwell (120 s), and (b) long dwell (1000 s).

numerical results [2]. SEM work shows no cavities in the vicinity of the crack tip or grain boundaries. The load-line displacement due to creep seems to be negligible and the ratio of displacement rate due to creep and total displacement rate is close to zero for steady-state crack growth under sustained load. Fig. 6 shows some encouraging correlation for slow-fast and fast-slow data at 725°C using the OST.

The loading waveform may have a bearing on the m-values, the exponent in Paris type of plots, $\mathrm{d}a/\mathrm{d}N = C\Delta K^{\mathrm{m}}$. Fig. 7 show the m values for different waveforms at 650°C, where lower values of m seem to be obtained for dwell loading cases, as opposed to triangular cases. However, at 725°C, the trend seems to be less clear. Insufficient data may be one of the reasons for the lack of correlation. Ideally, full $\mathrm{d}a/\mathrm{d}N$ vs. ΔK curves from constant load tests should be used for the evaluation, while the present data were obtained from two constant ΔK tests in the mid-range ($\sim$10 MPa$\sqrt{}$m). Further experimental results over a larger ΔK range are required to confirm this observation. Nevertheless, it seems plausible that hold at maximum load would prompt intergranular crack growth due to oxidation. The significant reduction in m values seems to indicate an enhanced intergranular crack growth towards an environment-assisted crack

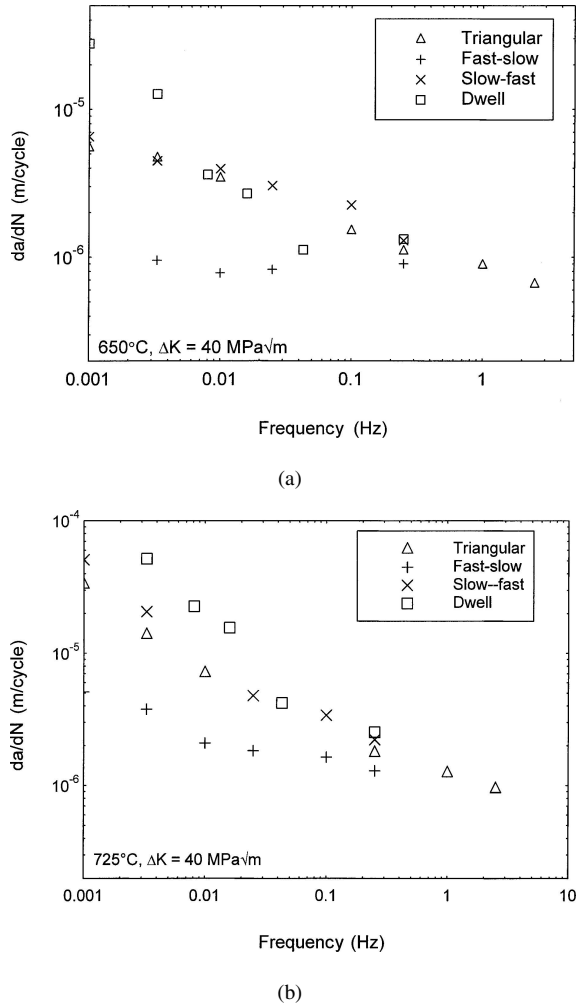

Figure 4 Fracture mechanism maps of Alloy *X* at (a) 650°C and (b) 725°C.

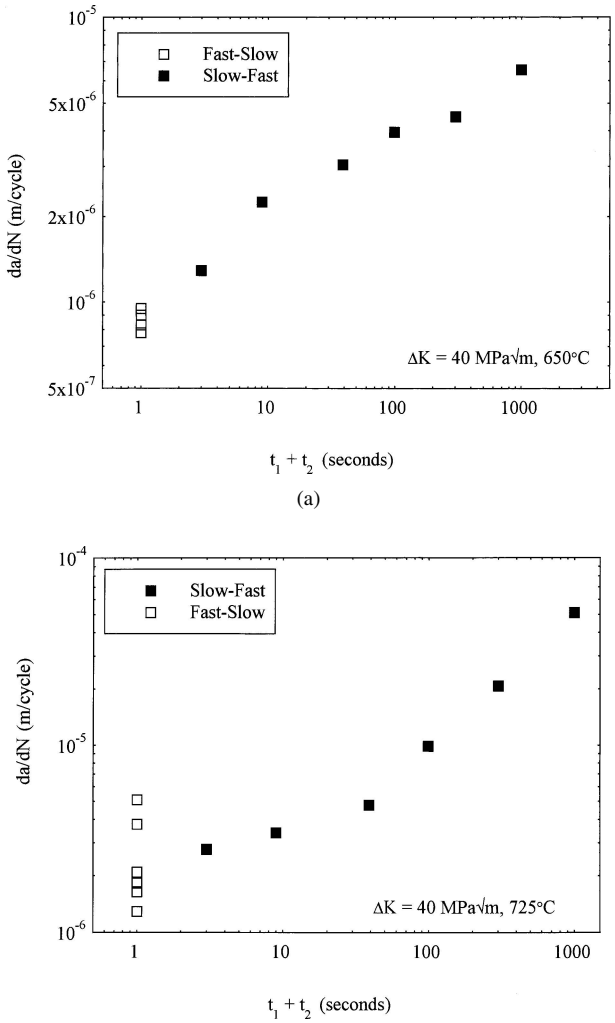

Figure 5 Loading time, $(t_1 + t_2)$, as a correlation parameter for fast-slow and slow-fast load cases at (a) 650°C and (b) 725°C.

growth, resemble the pattern of corrosion crack growth [16].

3.2. Effect of temperature

The effect of temperature was examined for all loading waveforms at 650 and 725°C. Fig. 8a presents the crack growth rate data from triangular waveform at a constant stress intensity factor range of 40 MPa$\sqrt{}$m. The increase in crack growth rate at 725°C seems to be constant when the OST is less than 10 s, above which the crack growth rate increases at a faster rate at 725°C than that at 650°C. The constant increase in crack growth rate with the temperature seems to scale with a $\exp(-Q/RT)$ function, where Q is the activation energy, estimated from a log (da/dt) vs. $(1/T)$ diagram as 241 kJ/mol for this alloy [3]; R is the universal gas constant and T is the temperature in Kelvin.

Another notable influence of temperature is the reduction in the m value. Fig. 8b shows the m values correlated with the OST for triangular data at 650 and 725°C. The reduction in m values at 725°C seems to be significant and independent of the OST. Further work may be carried out to investigate the phenomenon of weakened da/dN vs. ΔK correlation at higher temperature and lower frequencies, which seems to be typical of environmentally controlled crack growth behaviour.

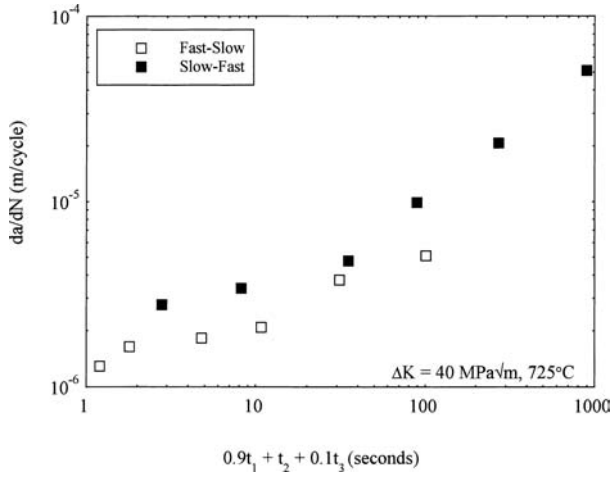

Figure 6 Oxidation sensitive time (OST) as a correlation parameter for fast-slow and slow-fast load cases at 725°C.

3.3. The model

The validity of ΔK characterization of crack growth in superalloys at elevated temperatures has been established using both experimental [1] and numerical analysis [2]. The influence of temperature may be depicted by an $\exp(-Q/RT)$ function and the oxidation sensitive time may be used to reconcile the crack

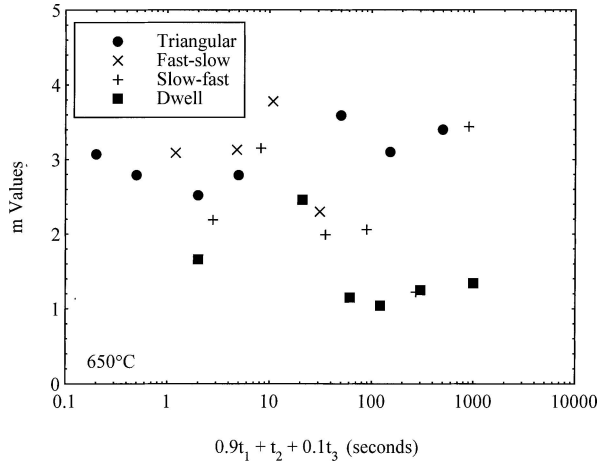

Figure 7 The influence of waveform on the m values in a Paris correlation at 650°C.

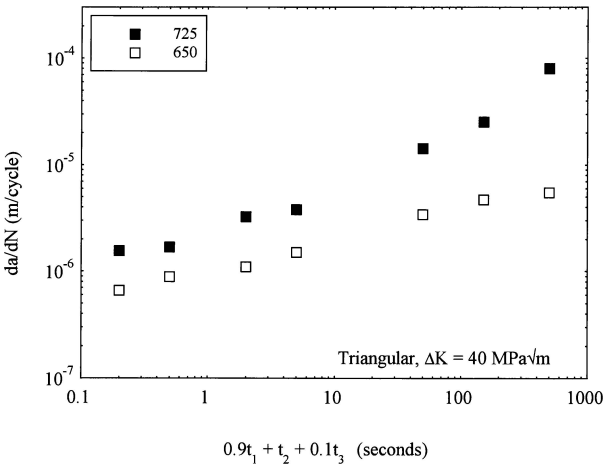

(a)

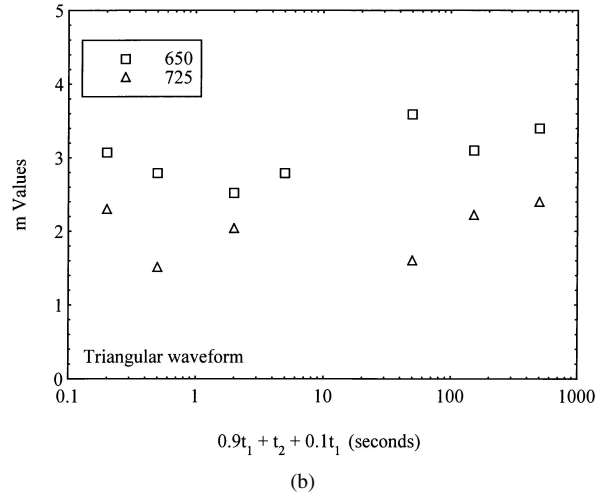

(b)

Figure 8 The effects of temperature on crack growth rates (a) crack growth for triangular load case at 650°C and 725°C; (b) the m-values as a function of OST for triangular and dwell load cases.

growth data from different loading waveforms at various loading rates. A general formula may be developed to accommodate these considerations:

$$\frac{\mathrm{d}a}{\mathrm{d}N} = C\exp\left(-\frac{Q}{RT}\right)\Delta K^{\mathrm{m}} \times (0.9t_1 + t_2 + 0.1t_3)^{[1/2-\xi]} \quad (1)$$

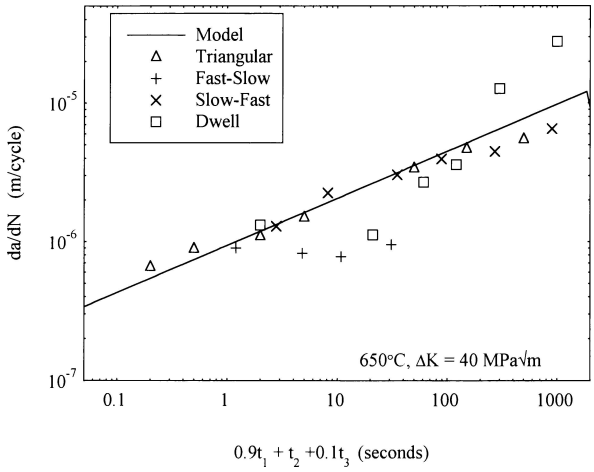

(a)

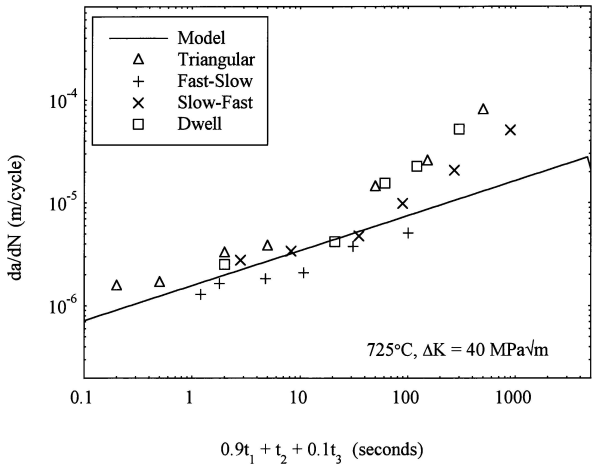

(b)

Figure 9 Comparison of model prediction and experimental results at (a) 650°C and (b) 725°C.

where C and ξ are temperature-independent constants while m is temperature dependent. For the present study, $C = 4 \times 10^3, \xi = 0.16$; average values of m are taken as $m = 2$ for 725°C and $m = 2.5$ for 650°C. The exponent $(1/2-\xi)$ is derived based on the assumption of parabolic oxygen penetration kinetics.

Fig. 9 shows the correlation of Equation 1 with the experimental data at 650 and 725°C. At 650°C, the model seems to correlate well with the triangular and slow-fast data for all the OST considered, but overestimates much of the fast-slow data. At 725°C, all the data seem to correlate reasonably well with the model at the OST less than 50 s, above which crack growth rates increase significantly towards fully time-dependent crack growth. The later is also true for dwell data at 650°C when the OST is longer than 100 s. Nevertheless, Equation 1 seems to be a reasonably good representation for the crack growth under varied waveforms in the mixed fracture regime.

4. Conclusions

Oxidation-driven crack growth appears to be the predominant fracture mechanism in the new nickel-based superalloy at 650 and 725°C. Scanning electron

microscopy seems to support the experimental results from mechanical testing and numerical results from finite element analysis. The effect of loading waveform on crack growth has been examined where an oxidation sensitive time has been adopted to model the rate-dependent crack growth. The positive correlation between the experimental results and the model response appears to be encouraging.

The results presented here seem to support further studies in order to develop a fundamental understanding of the physical processes of oxidation embrittlement during the crack propagation so that the rate controlling process can be described quantitatively.

Acknowledgements

The project was funded by the EPSRC (GR/M44811) and QinetiQ of the UK. Specimens were provided by Rolls- Royce plc. The authors wish to acknowledge the technical support from QinetiQ (Dr. M. B. Henderson and Prof. G. Harrison) and Rolls Royce plc. (Drs. M. C. Hardy and Ian Hussey).

References

1. S. DALBY and J. TONG, "Crack growth in a new nickel-based superalloy at elevated temperature," Part I: Effects of loading waveform and frequency on crack growth.
2. L.-G. ZHAO and J. TONG, "Crack growth in a new nickel-based superalloy at elevated temperature," Part II: Finite element analysis of crack growth.
3. J. TONG, J. S. DALBY, J. BYRNE, M. B. HENDERSON and M.C. HARDY, *Int. J. Fatigue* **23** (2001) 897.
4. R. MOLINS, G. HOCHSTETTER, J. C. CHASSAIGNE and E. ANDRIEU, *Acta Metall.* **45** (1997) 663.
5. H. GHONEM and D. ZHENG, *Fatigue Fract. Engng. Mater. Struct.* **14** (1991) 749.
6. P. VALERIO, M. GAO and R. P. WEI, *Scripta Metall.* **30** (1994) 1269.
7. T. WEERASOORIYA, ASTM STP 969, 988, p. 907.
8. D. A. WOODFORD and R. H. BRICKNELL, "Environmental Embrittlement of High Temperature Alloys by Oxygen" (Treatise on Materials Science and Technology, Academic Press Inc., 1983) Vol. 25, p. 157.
9. S. DALBY, Ph.D Thesis, University of Portsmouth, 2001.
10. E. ANDRIEU, R. MOLINS, H. GHONEM and A. PINEAU, *Mater. Sci. Eng.* A**154** (1992) 21.
11. C. A. HIPPSLEY and J. H. DEVAN, *Acta Metall.* **37** (1989) 1488.
12. C. A. HIPPSLEY and M. STRANGWOOD, *Mater. Sci. Tech.* **8** (1992) 350.
13. H. GHONEM and D. ZHENG, *Mater. Sci. Eng.* A **150** (1992) 151.
14. J. TONG and J. BYRNE, *Fatigue Fract. Engng. Mater. Struct.* **22** (1999) 185.
15. J. TONG, J. S. DALBY and J. BYRNE, Fatigue 2002, EMAS, p. 2401.
16. R. W. HERTZBERG, "Deformation and Fracture Mechanics of Engineering Materials," (John Wiley & Sons, Inc., 1996).

Received 8 October 2003
and accepted 24 September 2004